

An Experimental Objective Analysis in the Tropics

By
Michio Yanai

Technical Paper No. 62
Department of Atmospheric Science
Colorado State University
Fort Collins, Colorado



**Department of
Atmospheric Science**

Paper No. 62

AN EXPERIMENTAL OBJECTIVE ANALYSIS IN THE TROPICS

By Michio Yanai*

Technical Paper No. 62
Department of Atmospheric Science
Colorado State University

October 1964

*On leave of absence from Meteorological Research Institute, Tokyo

ABSTRACT

A version of the "correction" objective map analysis scheme has been developed and tested for the surface meteorological elements and the upper-air winds in the Caribbean region. The system is basically the same as that described by Cressman (1959). However, in order to overcome the difficulty of getting reasonable analysis over the oceanic area devoid of data, a successive vertical differential analysis technique has been employed for the upper wind analysis. Surface map analysis serves to obtain a reliable base for the upper wind analyses.

Analysis of wind fields both at the surface and at upper levels is independent from pressure or height of constant -- pressure surface -- observations. However, as suggested by Masuda and Arakawa (1962), a statistical adjustment process was introduced to improve the surface pressure analysis with assistance from the independent wind analysis. For the upper wind analyses, vertically averaged winds over 50-or 100-mb pressure intervals were used.

Besides a general description of the correction method employed, some technical problems in handling operational data are mentioned. In upper wind analysis, special caution is needed to insure a reasonable analysis over wide open areas without stations. It has been found that the correction method tends to build a peculiar distortion of analyzed pattern in these areas. A simple method to detect the possible distortion is analyses of latitudinal and longitudinal coordinates from latitude and longitude data at the observation stations only.

The results based on the experimental computations are illustrated with charts and discussed with some statistical results.

1. INTRODUCTION

The major purpose of this study has been to explore the feasibility of objective analysis techniques on the basis of currently (1964) available operational network in the tropics. As a first trial, such analysis has been conducted over the Caribbean region where the upper-air observational network is, if not very satisfactory, at least comparatively dense. An attempt to analyze upper winds objectively over the tropical Pacific has been reported by Bedient, et al. (1964). Rosenthal and his colleagues at the National Hurricane Research Project, U. S. Weather Bureau have been working on a scheme of objective analysis for the height data of isobaric surfaces in the Caribbean. Figure 1 shows the locations of the operational rawin-sonde and pibal stations within a rectangular area bounded by the latitudes 0 and 52 N, and the longitudes 48 and 112 W. Glancing at the distribution of the stations, we notice quite an unbalanced concentration of stations over North America. In contrast, there are regions completely without stations, especially the Atlantic south of Bermuda and Weather Ship "E" and the Gulf of Mexico.

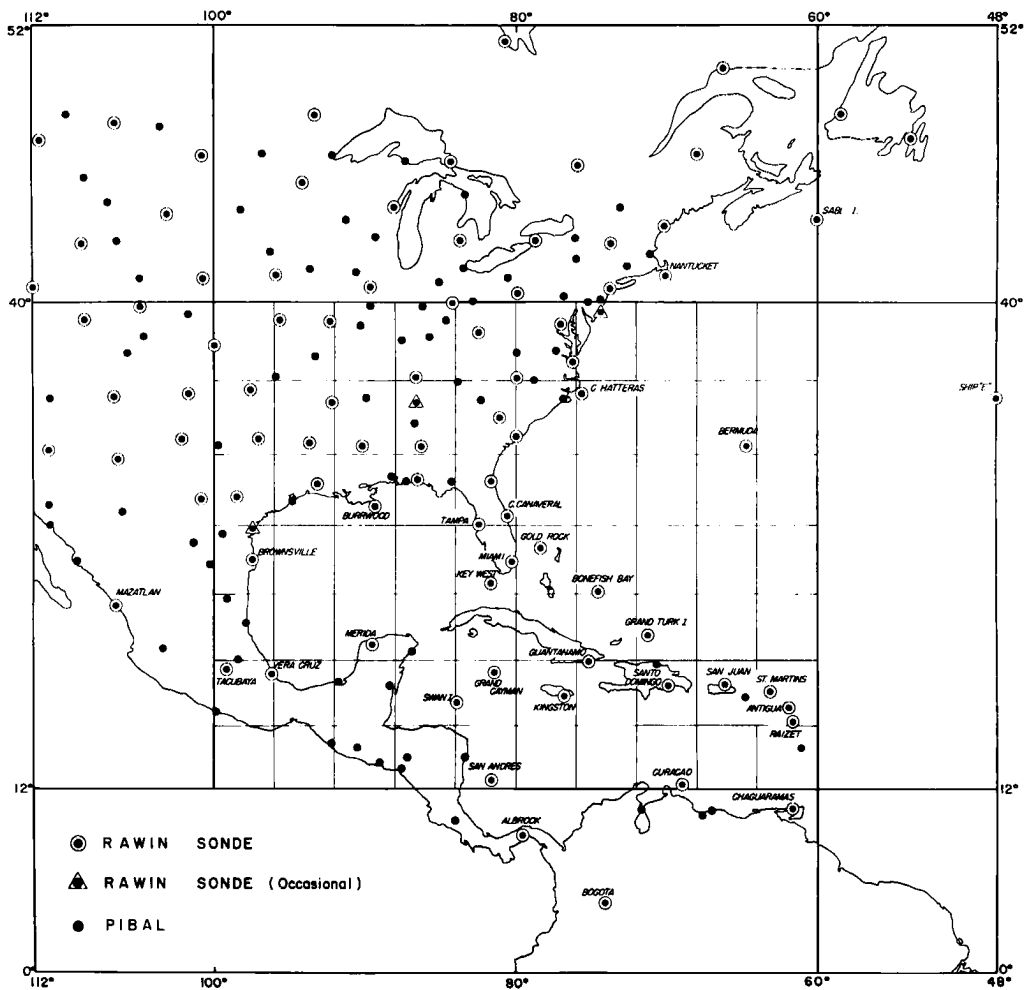


Fig. 1 The grid system and upper-air observation stations.

In order to overcome the difficulty of upper-level analysis due to the poor distribution of stations, surface analysis was performed first to establish a series of base charts from relatively abundant land and ship reports. Then, by employing successive differential analysis, the wind field at upper levels was gradually built up.

Basically, two types of objective weather map analysis have been used. One of these is the "fitting" of locally defined mathematical surfaces expressed by a polynomial by least squares to the data (Panofsky, 1949). This method, however, has certain shortcomings for meteorological purposes. Even for determination of a quadratic surface we need at least six independent observations in the vicinity of a grid point at which we compute the coefficients of the quadratic formula. In many cases, we simply do not have six observations located closely enough to the grid point. Even when there are enough data points, the determinant of matrix in the least-square computation at times becomes very small, thus making the computation unstable.

In this study, we have employed a version of the "correction" method originally proposed by Bergthórsson and Döös (1955) and expanded by Cressman (1959). The scheme starts from a best available first guess field given at every grid point. Then, using data, successive corrections are applied on the previous guess field until a reasonably close coincidence between observations and analyzed values at the grid points is realized.

In principle, the scheme can be applied for any meteorological elements at any levels. However, by considering the poor data distribution mentioned before, successive vertical "differential" analysis was used for the upper-wind analysis. Such differential analysis was first employed by Masuda and Arakawa (1962). Additional technical details which required further present study will be discussed in the following sections.

The aim has been to develop synoptic-scale map analysis within the region covering 12-40 N and 60-100 W (the "inner" area). However, in order to insure a fit on the boundaries, the analysis has been curved out over the area 0-52 N, 48-112 W (the "whole" area). Grid points are placed at 4° - latitude and longitude intersection. Therefore, there are $17 \times 14 = 238$ grid points in the whole area. Only the grid points within the inner area are reproduced in Figure 1. The size of the grid interval is comparable with the average distance between the upper-air stations in the Caribbean. This distance is considered to be acceptable from the viewpoint of resolution of a wave disturbance in the Caribbean with wave length of 15-20 degrees longitude.

2. ANALYSIS OF SURFACE DATA

2.1 Preparation of the Surface Data

Data used in this experimental study was taken from standard teletype reports received at the District Meteorological Office, U. S. Weather Bureau, Miami, Florida. Supplementary data was obtained from the Northern Hemispheric Data Tabulation of the National Meteorological Records Center (12GCT only). For seven map times used in the study, the number of reports was as shown in Table I.

TABLE I Numbers of Surface Meteorological Reports

	land stations	ships	total
Aug. 21, 00GCT, 1962	327	97	424
" " 12GCT, 1962	384	131	515
Aug. 22, 00GCT, 1962	309	80	389
" " 12GCT, 1962	371	182	553
Aug. 23, 00GCT, 1962	326	104	430
" " 12GCT, 1962	374	186	560
Aug. 24, 00GCT, 1962	340	119	459

From punched data of coded SYNOP and SHIP reports, a sorting program identifies a land station number with a stored station dictionary in the program and supplies the latitude and the longitude of the station. For ship reports, the location of a ship is given as a part of punched data. Then the program processes the pressure, the temperature, the dew-point temperature, the wind direction and wind speed from coded forms to decimal numbers. During the processing, mixed units of temperature and dew-point reports are converted to degrees C. The program detects duplication of data and rejects some obviously erroneous data. The finally processed data are: a station (or ship) identifier, latitude ϕ , longitude λ , pressure p , temperature T , dew-point temperature T_d , eastward and northward components of wind u , v . These data are arranged and stored on magnetic tape.

2.2 The Correction Method

General Outline:

Let us assume that we have the ν -th iterative guess of some meteorological elements $S_g^{(\nu)}$ at every grid point. From given array of $S_g^{(\nu)}$, we first compute an interpolated value at a station S (see Figure 2). From nearby four grid points, a bilinear interpolation formula

$$I_s^{(\nu)} = S_g^{(\nu)}(1) + x [S_g^{(\nu)}(2) - S_g^{(\nu)}(1)] + y \left[\left(S_g^{(\nu)}(3) - S_g^{(\nu)}(1) \right) (1-x) + \left(S_g^{(\nu)}(4) - S_g^{(\nu)}(2) \right) x \right] \quad (1)$$

determines the interpolated value $I_s^{(\nu)}$ at the location of the observation station S . In formula (1), x and y are expressed in fractions of the mesh size $d=4$ degrees.

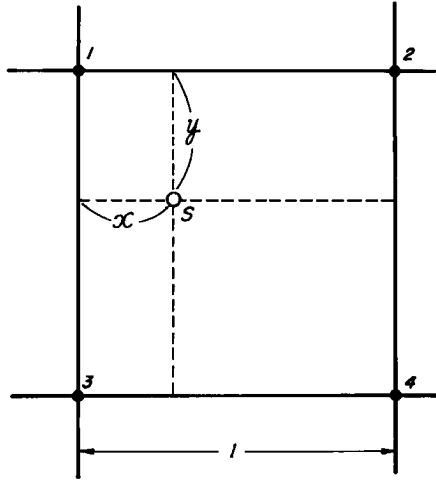


Fig. 2 Interpolation from field values at nearby 4 grid points to the location of station S.

Next we compute the error $E_s^{(\nu)}$ between the interpolated value $I_s^{(\nu)}$ and the actual observation O_s ,

$$E_s^{(\nu)} = O_s - I_s^{(\nu)}. \quad (2)$$

$E_s^{(\nu)}$ gives a correction to a nearby grid point to get the $(\nu + 1)$ th iterative value. Taking into account all the available corrections within a certain sphere of influence, we make a composite correction on the grid point by

$$C_g^{(\nu+1)} = \frac{\sum_s W_s^{(\nu)}(\gamma) E_s^{(\nu)}}{\sum_s W_s^{(\nu)}(\gamma)} \quad (3)$$

Here $W_s^{(\nu)}(\gamma)$ is a weighting factor which is determined by the distance γ between the grid point and the considered station. The summation is made over all the existing corrections within the radius $\gamma_m^{(\nu)}$ from the grid point G (see Figure 3).

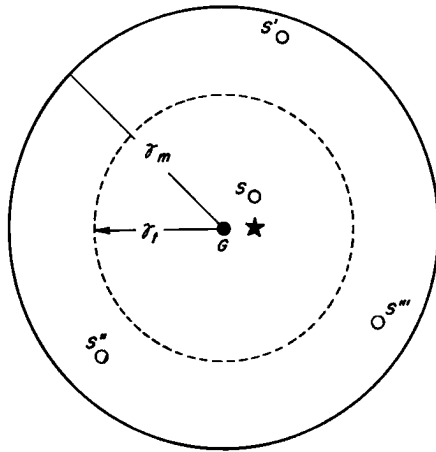


Fig. 3 Sphere of influence (radius γ_m) for a composite correction referred to grid G. The center of gravity ★ of stations S, S', --- must fall within the radius γ_t .

Then the next iterative guess at the grid point G is obtained by

$$S_g^{(\nu+1)} = S_g^{(\nu)} + C_g^{(\nu+1)} \quad (4)$$

The new values of $S_g^{(\nu+1)}$ will be used to determine the next iterative values of $I_s^{(\nu+1)}$ and $E_s^{(\nu+1)}$ at the data points. The entire scheme (1) - (4) will be repeated successively until we get a reasonably small value of $E_s^{(\nu)}$ at all the data points.

There are certain degrees of freedom in the scheme. The fundamental parameters which define the analysis scheme are:

- ν max - - numbers of iterations
- $\gamma_m^{(\nu)}$ - - searching radius from a grid point to get a composite correction
- $W^{(\nu)}(\gamma)$ - - the weighting factor for each iteration

In addition, the result of the analysis depends upon the first guess $S_g^{(0)}$. As suggested by Cressman, 1959, $\gamma_m^{(\nu)}$ is gradually decreased for successive iterations. Naturally, for grid points densely surrounded by many observation points, the decreasing radius eventually gives a better resolution. For grid points poorly surrounded by few observation points, initial few iterations may improve the analysis and make a minimum required correction for the largest scale error contained in the first guess.

Smoothing Operation:

Although the formulas (1) - (4) make a complete closed system as the correction method, some modifications were needed in actual computations. As the weighting factor $W_s^{(\nu)}(\gamma)$ depends only on the relative distance between a station and a grid point, some considerations on the spatial distribution of stations to a grid point were made. In order to avoid a composite correction determination by poorly located observations, two restrictions are imposed upon the computation. First, there must be at least three data points to determine a composite correction at every iteration. Second, the center of gravity of data locations must fall within the radius $\gamma_t^{(\nu)} = 0.6 \gamma_m^{(\nu)}$ at each iteration (see Figure 3).

If either one of these requirements is not satisfied, the nearby grid values already determined in the iteration are added as auxiliary data. Thus, for this case

$$C_g^{(\nu+1)} = \frac{\sum_s W_s^{(\nu)} E_s^{(\nu)} + \sum_{g'} G^{(\nu)} W_{g'}^{(\nu)} [S_{g1}^{(\nu)} - S_{g'}^{(\nu)}]}{\sum_s W_s^{(\nu)} + \sum_{g'} G^{(\nu)} \cdot W_{g'}^{(\nu)}} \quad (3)'$$

Here $G^{(\nu)}$ is a relative weight of these additional data to the actual observations. G is varied according to the iterations, by considering possible numbers of grid points involved.

The use of (3) allows the analysis scheme to perform a smoothing operation in the poorly observed areas, where the determination of a grid value solely from few stations is sometimes dangerous.

The Weighting Factor:

The shape of weighting factor has been changed considerably during the experiments. To obtain flexibility and also machine time economy, a step function defined by

$$\begin{aligned} W(\gamma) &= \exp(-b\gamma^2), \text{ for } \gamma \leq \gamma_m \\ W(\gamma) &= 0, \text{ for } \gamma > \gamma_m \end{aligned} \quad (5)$$

has been used. γ is the integral part of γ which is the distance between a data point and a grid point measured in degrees. Namely $\gamma^2 = (\Delta\lambda)^2 + (\Delta\phi)^2$. $\Delta\lambda$ and $\Delta\phi$ are longitudinal and latitudinal distances respectively. A table of $W(\gamma)$ is computed at the beginning of each iteration and indexed from actual values of γ^2 .

Obviously, if we take a large value of b , we get a sharp decrease of the weighting factor with increase of γ , which yields fine resolution of the analysis. However, after several experiments, we discovered that too fine a resolution is not necessarily desirable. Especially for the surface pressure analysis, an overly sensitive analysis scheme tends to lead to considerable small-scale fluctuation. This is particularly true for oceanic areas where ship reports are sometimes of questionable quality. Too fine a resolution for the surface wind is also not desirable, because of small-scale sea-breeze and orographic effects involved in the surface wind reports.

Finally we arrived at the conclusion that a constant weight factor $W(\gamma) = 1.0$ is suitable for the final iteration with $\gamma_m = 3.0$ degrees.

A tentatively chosen set of the parameters for the surface analysis is shown in Table 2.

TABLE 2 The Parameters Used for the Surface Analysis

ν	$\gamma_m^{(\nu)}$	(γ_m/d)	b	G
1	8.0 degrees	(2.0)	0.08	0.20
2	6.0	(1.5)	0.06	0.40
3	4.0	(1.0)	0.04	0.60
4	3.0	(0.75)	0.00	0.80

The shape of the stepped weighting factors for each iteration is shown in Figure 4.

The First Guess:

The above mentioned analysis scheme was applied to (1) surface pressure, (2) temperature, (3) dew-point temperature, (4) scalar wind velocity, (5) u (eastward component of wind), and (6) v (northward component). Scalar wind was computed to detect possible errors in the data prior to the analysis of the wind components. The analyzed u and v fields were converted into vector resultant wind.

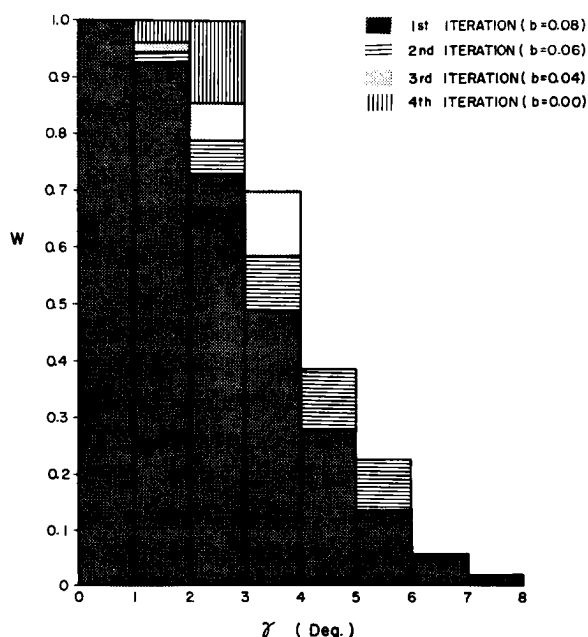


Fig. 4 The stepping weighting functions used at each iteration for the surface analysis.

Objective analysis at the preceding map time served as first guess for these fields.

TABLE 3 The First Guesses for the Surface Objective Analysis

elements	first guess
p	analyzed values (-12 hrs)
T, T _d	analyzed values (-24 hrs)
V , u, v	analyzed values (-12 hrs)

For the pressure and the wind analyses, analyzed grid values at the closest preceding map time were considered to be the best for this diagnostic experimental analysis. However, the first guesses for the temperature and dewpoint analyses were taken from the analysis 24 hours earlier in order to avoid diurnal variations.

The Data Checking System:

In handling large numbers of operational data, a few erroneous reports are inevitably involved. Although some of the obvious errors have been removed in the previous sorting program, all the data read from the magnetic tape is again checked by the analysis program. The data are doubly checked by setting two kinds of empirical criteria for each of the meteorological elements. First, if too large value of $E_s^{(\nu)}$ is found, the corresponding data is rejected as erroneous. Second, the observation O_s will be compared with its neighbors. If it differs from the neighboring observations excessively, the data is rejected.

The maximum permissible differences for each element used for both tests are shown in Table 4.

TABLE 4 Maximum Permissible Differences between Data and the Interpolated Field Values or Neighboring Data

ν	p (mb)	T (°C)	T _d (°C)	$ \mathbf{V} , u, v$ (m/s)
1	19.9	19.9	29.9	25.0
2	15.0	15.0	22.5	19.0
3	9.9	9.9	15.0	12.5
4	9.9	9.9	15.0	12.5

2.3 Modification of the Surface Pressure Analysis by the Wind Analysis

Originally, the analyses for the pressure and the wind were made independently. It was found, however, that small-scale irregularities in the pressure analysis appeared in the oceanic regions even after the smoothing operation was performed. This was mostly because of inaccurate ship reports. As is usually done by skilled subjective analysts, some considerations of the wind field are needed to improve the pressure analysis.

As used by Masuda and Arakawa (1962), an adjustment process between the pressure and wind analysis was introduced in a statistical sense. As the simplest possible relationship between the pressure gradient and the surface wind, Gudberg-Mohn type formulas

$$\left. \begin{aligned} \alpha (ku - fv) &= - \frac{1}{\bar{\rho} a \cos \phi} \frac{\partial p}{\partial \lambda} \\ \alpha (fu + kv) &= - \frac{1}{\bar{\rho} a} \frac{\partial p}{\partial \phi} \end{aligned} \right\} \quad (6)$$

are used to modify the gradient of pressure according to the analyzed wind field. Here k is a frictional coefficient, f the Coriolis parameter, $\bar{\rho}$ the average density of the surface air, a the earth's radius. A purely empirical factor α was introduced to get a balance between actual wind velocity and the horizontal gradient of pressure. Assuming $\partial p / \partial \lambda = 0$, we readily obtain

$$\begin{aligned} |\mathbf{W}| &= \frac{1}{\alpha \sqrt{1 + \left(\frac{k}{f}\right)^2}} \cdot |\mathbf{W}_{ge}| \\ \frac{v}{u} &= \frac{k}{f} = \tan \theta \end{aligned} \quad (7)$$

where $|\mathbf{W}_{ge}|$ is the geostrophic wind velocity, θ is the angle between the wind vector and the isobar. Tentatively adopted values of k and α are $20.0 \times 10^{-6} \text{ sec}^{-1}$ and 1.2 respectively.

It should be remarked that the formula (6) is used only in a statistical sense to modify the previously analyzed pressure gradient. Namely, from a neighboring grid point j at which both the wind components and the pressure are already obtained, a new correction at the grid point g is computed by

$$C_j = p_j - \frac{\alpha}{2} \rho a \Delta \lambda \cos \phi [f(v_g + v_j) - k(u_g + u_j)] \\ + \frac{\alpha}{2} \rho a \Delta \phi [f(u_g + u_j) + k(v_g + v_j)] - p_g \quad (8)$$

A composite correction on the grid point g is then made by

$$C_g = \frac{\sum_j R_j C_j}{\sum_j R_j} \quad (j = 1, 2, 3, 4) \quad (9)$$

where $R_j = \frac{L_j + 1}{L_g + 1}$, L_j and L_g are the numbers of data previously used to determine the preliminary pressure values at the grid points j and g respectively. Thus, the correction depends also on the relative density of data in space used in original pressure analyses.

2.4 Examples

An example of analyzed pressure (adjusted to wind) is shown in Figure 5. Locations of data points are shown by black dots. A corresponding conventional subjective analysis of pressure made at the District Meteorological Office, U. S. Weather Bureau, Miami is reproduced in Figure 6 for comparison. There are no large differences between the two analyses.

Figure 7 and 8 are examples of temperature and dewpoint analysis respectively. Effects of the distribution of land and water are clearly evident.

After extensive comparisons between the objective analyses and hand analyses made by the author, results of the objective analysis were generally considered to be better than the subjective analysis in regard to the horizontal gradients of the analyzed meteorological fields.

Figure 9 shows an example of analyzed vector resultant winds at the inner grid points. Original observations are also plotted in the figure. Except for few grid points in the vicinity of very light winds, agreement between the observations and the analyzed winds seem to be reasonably good.

Figure 10 shows the same wind field as Figure 9; streamlines and isotachs have been drawn to show the flow pattern. The figure shows good resolution of shear lines, vortices, saddle points and waves.

The total machine time needed to get a complete set of surface analysis for pressure (preliminary), temperature, dew-point temperature, scalar wind velocity, u and v components, vector resultant winds and the modified pressure with additional statistical computations was 5 minutes per one map time by CDC-3600.

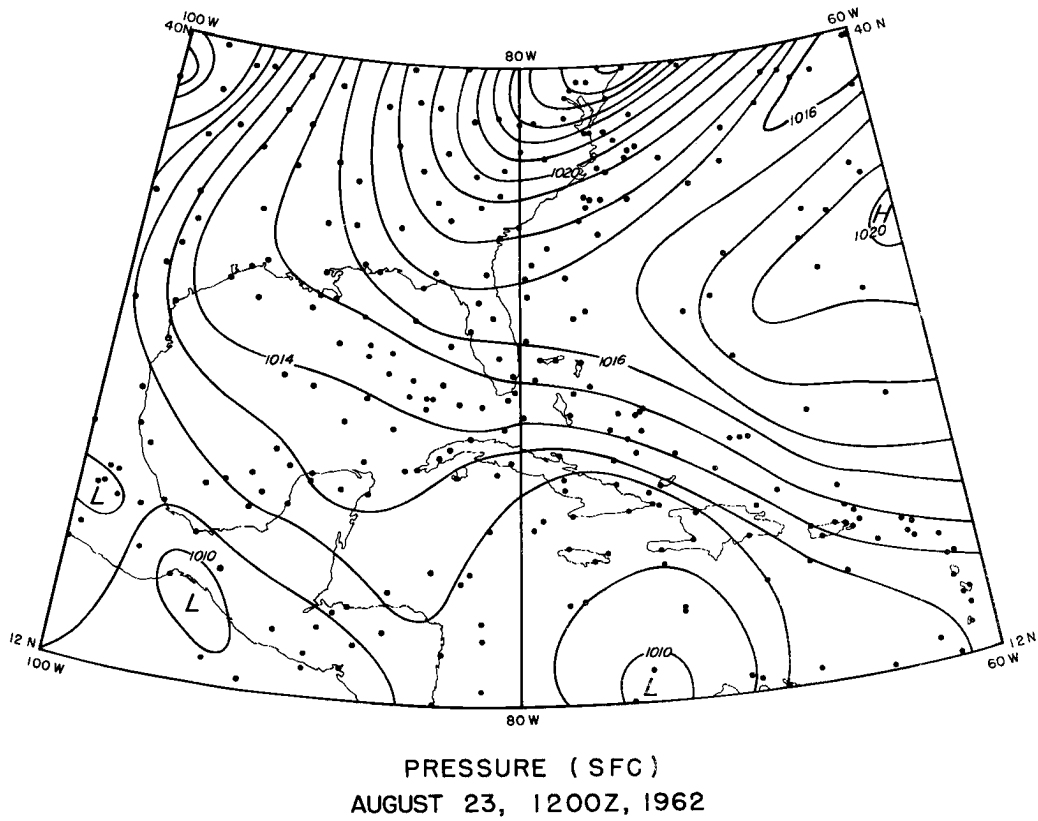


Fig. 5 Objective analysis of surface pressure. Black dots show the locations of data.

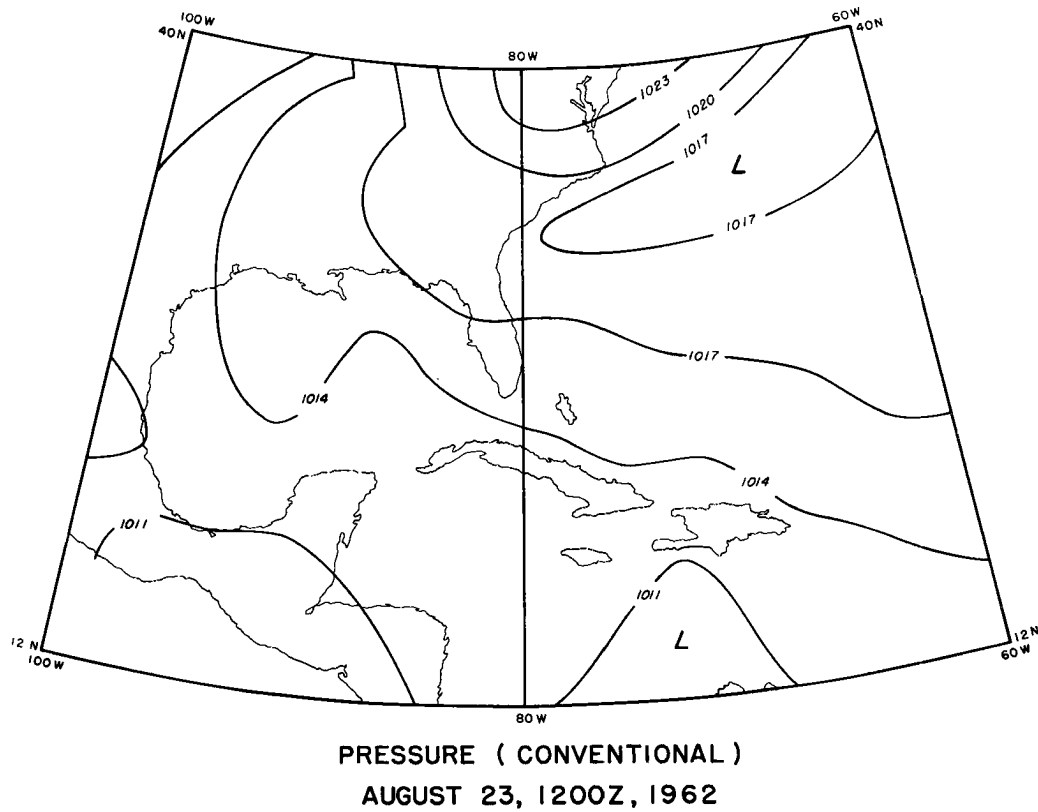
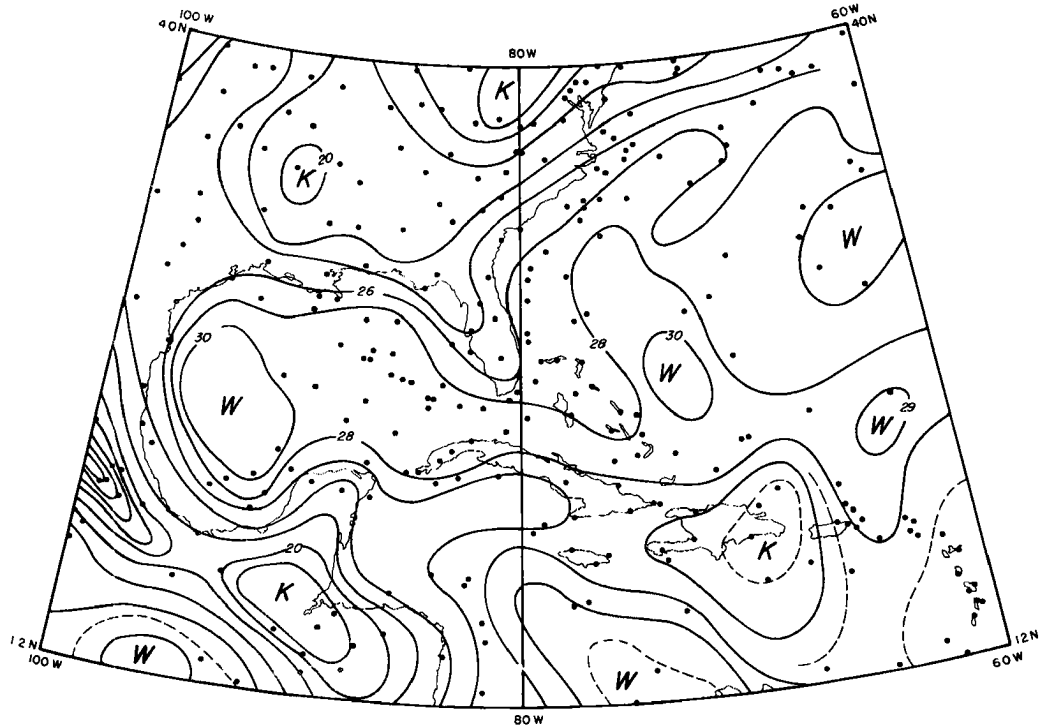


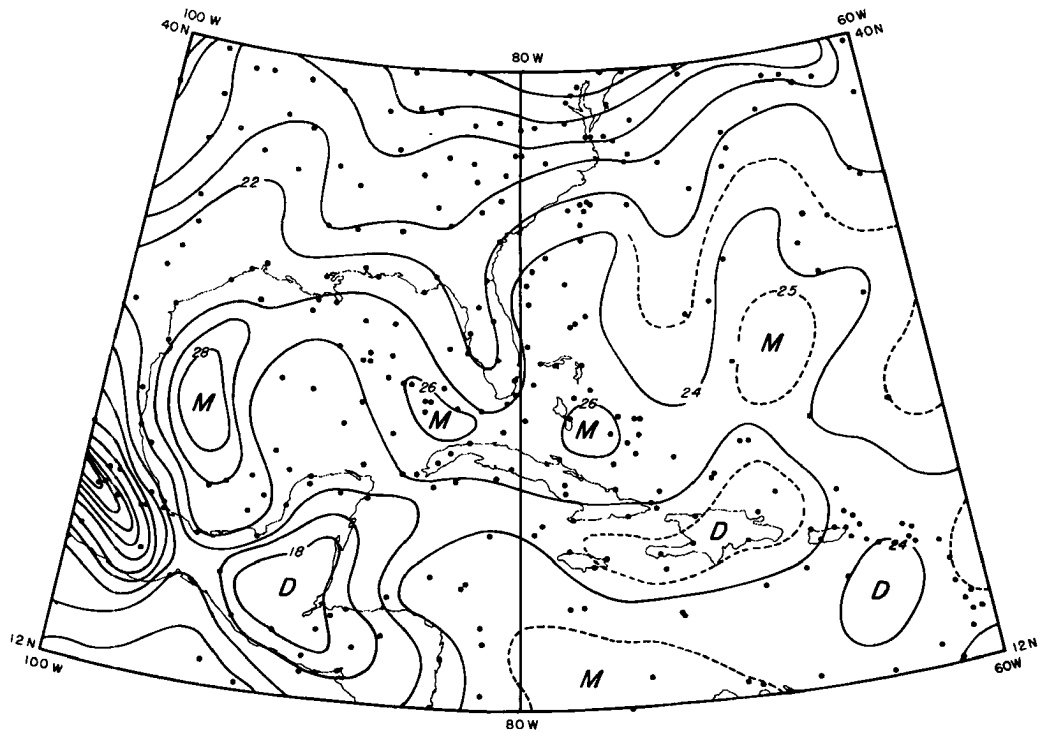
Fig. 6 Conventional analysis of surface pressure.

Fig. 6 Conventional analysis of surface pressure.



TEMPERATURE (SFC)
AUGUST 23, 1200Z, 1962

Fig. 7 Objective analysis of surface temperature.



DEW POINT TEMPERATURE (SFC)
AUGUST 23, 1200Z, 1962

Fig. 8 Objective analysis of surface dew-point temperature.

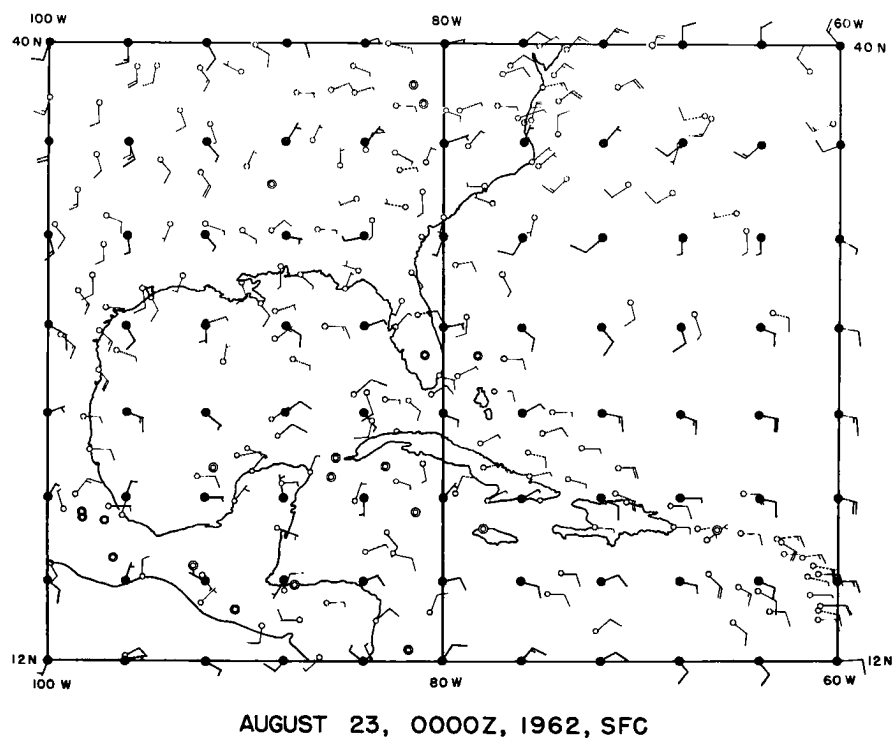


Fig. 9 Objective analysis of surface resultant vector wind. Arrows at black circles show the analyzed winds. Arrows at small open circles show the data.

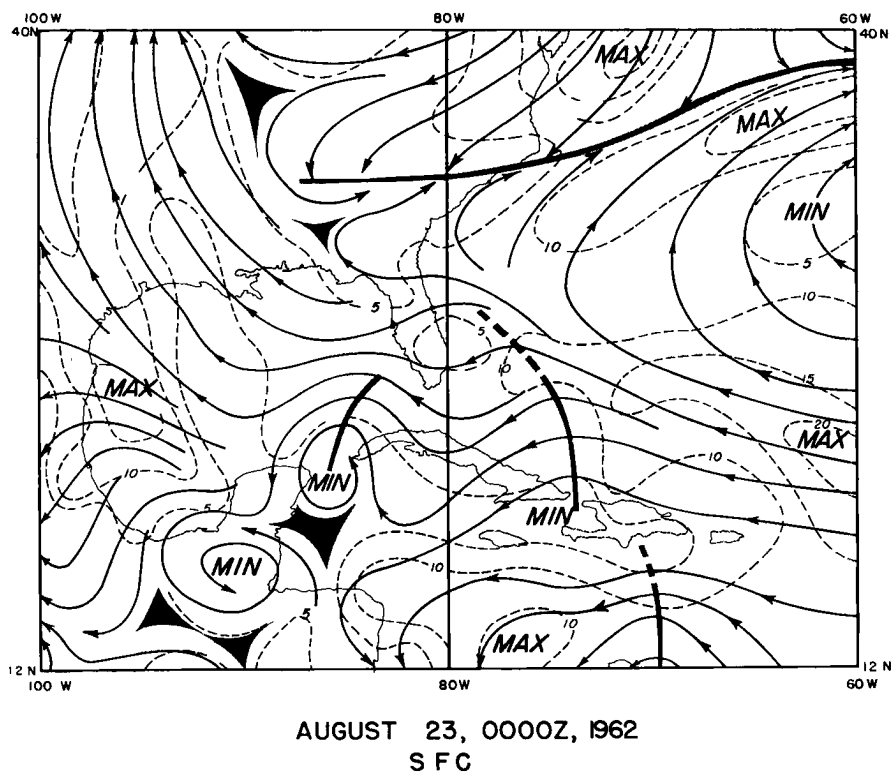


Fig. 10 Streamlines and isotachs (kts) based on the objective surface wind analysis.

2.5 Statistical Results

For the six cases, except for the first one which was generated from a different set of first guesses, the average correlation coefficients and the average root mean square errors between observations and $I_S^{(4)}$ are computed and listed in Table 5.

TABLE 5

Comparison between Observations and Interpolated Values at the Location of Data Points

elements	correlation coefficient	r. m. s. errors
p	0.967	1.07 mb
p* (modified pressure)	0.962	1.17 mb
T	0.949	1.79 °C
T _d	0.947	1.94 °C
W	0.743	3.68 kts
u	0.814	2.00 m/s
v	0.773	1.97 m/s
W *	0.693	3.94 kts

(|W|* - scalar velocity of the vector resultant wind)

These values were based on computation for all data points within the whole analysis area.

A slight decrease of the correlation coefficients and a slight increase of the root mean squares occurs when the pressure analysis is modified by the wind analysis. Relatively low values of the correlation coefficients and relatively large values of the root mean squares in the wind analysis are the results of small-scale irregularities contained in the wind reports which are beyond the resolution of the analysis scheme.

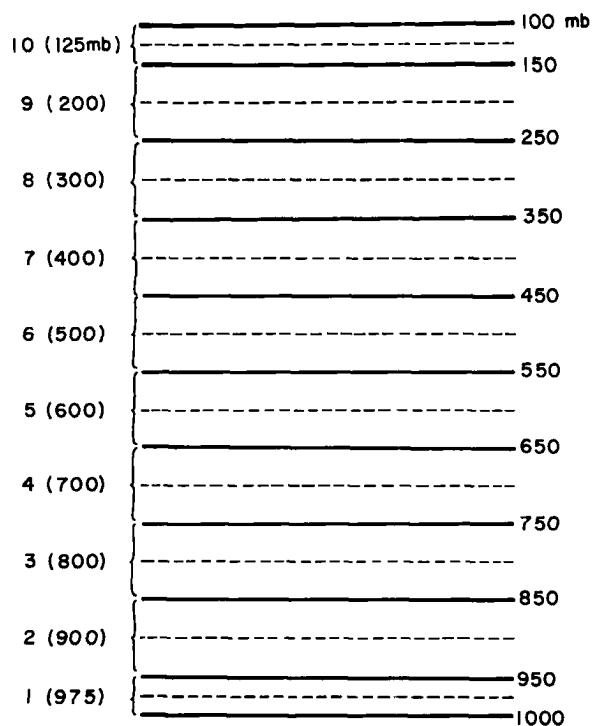
Large correlations and small root mean squares are not necessarily desirable when we consider the quality of the surface reports. Furthermore, this sort of statistical computations, which are merely made at the locations of existing data, is by no means satisfactory for evaluation of the analysis scheme. There is no way to evaluate the merits or defects of the analysis scheme over the poorly observed areas. This problem will be more clearly revealed in discussing the upper-wind analysis.

3. ANALYSIS OF THE UPPER-LEVEL WINDS

3.1 Preparation of the Upper-Level Wind Data

From the teletype upper-wind reports at all the rawin-sonde and pibal stations shown in Figure 1, all pieces of information are converted into 10 layer-mean winds for each station (see Figure 11). Each of the layer-mean winds is the vertically averaged wind over a 100 or 50 mb pressure interval. In the conversion process, an elevation-pressure relationship based on Jordan's (1958) mean tropical atmosphere for the hurricane season was used.

Fig. 11 Ten levels used to compute mean-layer winds.



Besides the regular stations and the Weather Ship "E", a few pilot balloon observations were available from ships. In addition, all aircraft winds reported from 12 hours before to the map time were utilized. These reports were assigned to the nearest constant pressure level. In Table 6, numbers of upper-wind reports utilized are shown.

TABLE 6 Numbers of Upper-Wind Reports

map time	land stations	ships	flight data	total
2100	142	2	44	188
2112	137	2	0	139
2200	137	3	18	158
2212	140	4	20	164
2300	148	4	20	172
2312	127	7	12	146
2400	144	3	12	159

For missing reports at several key stations like Bermuda, off-time data taken six hours before the map time were substituted with a reduced weight factor. Six-hour off-time data of all the ships were also utilized to supply the data in wide oceanic areas.

The sorting program for the upper-wind data is otherwise similar to that of the surface data sorting. Besides, the program checks the vertical consistency of the reported upper-level wind for each station.

3.2 Outline of the Upper Wind Analysis

The Vertical Differential Analysis:

A correction method basically identical with the one described earlier was applied for the upper-level wind analysis. A unique feature of the upper-wind analysis program is that the program performs the analysis of the scalar wind velocity, u and v components and the vector resultant winds at the 10 levels successively from below by employing a series of vertical differential analysis.

The analysis of the lowest level wind field at 975 mb starts from the first guess which is the average of the already analyzed surface wind field of the same map time and the 975 mb level wind field at the preceding map time. Then the program analyzes the vertical wind shear between the 900 mb and the 975mb levels starting from the shear field at the same layer at the preceding map time. If wind data exist at both levels at all the stations, the addition of the vertical shear field to the 975 mb wind field should give the 900 mb wind field. However, since several types of data exist only at higher levels (for example, aircraft data), the preliminary 900 mb level wind field is further revised from all available 900 mb wind data. The same process continues up to 125 mb.

Iterations, Weighting Factors:

For each of the analyses of the vertical shear field and the revised analysis of the level wind, three iterations have been applied with the following specifications.

TABLE 7 Parameters Used for the Upper-Wind Analysis

ν	γm	$(\gamma m/d)$	b	G	Maximum permissible diff.
1	16.0 degree	(4.0)	0.10	0.20	100 m/s
2	10.0	(2.5)	0.09	0.30	90 m/s
3	6.0	(1.5)	0.08	0.40	80 m/s

Therefore, except for the 975 mb level, practically six iterations have been applied for each of the upper-level fields.

The shapes of the weighting factors are much sharper than those used in the surface analysis (see Figure 12). This is because the layer-mean winds employed in the upper-level analysis are more reliable than the surface winds. Thus we desire to fit the analyzed winds at grid points as exactly as possible to the observations.

Besides, the γt is set equal to 0.5 γm for the upper-wind analysis. This is related to the problem described in the following section.

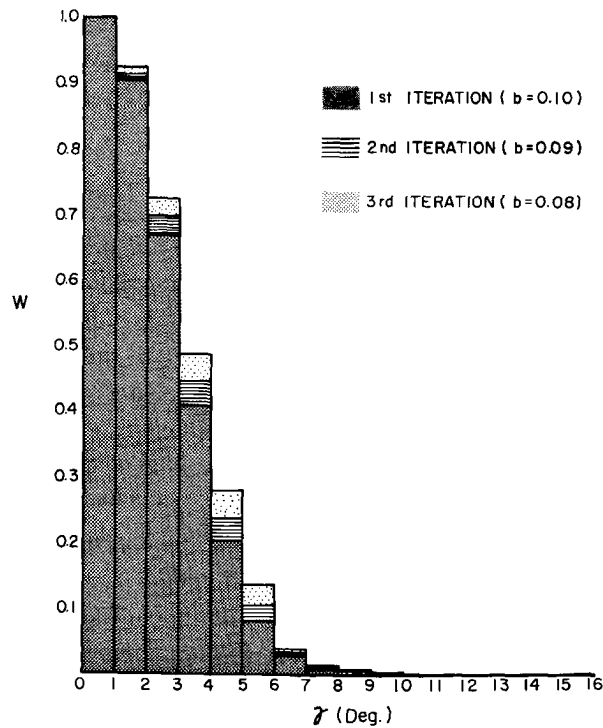


Fig. 12 Weighting functions used for the upper-wind analysis for each iteration.

3.3 The Removal of Possible Distortions of the Analyzed Results over the Poorly Observed Area

As mentioned in 3.2, relatively large values of b have been used in the upper-wind analysis to get a better fitting of the analyzed wind field where observations are scarce. Nevertheless, in the initial experiments, peculiar distortions were introduced into the analyzed wind fields, particularly in the wide blank area south and southeast of Bermuda.

These distortions resulted from computations based upon data points that were too remote. Because there was no way to evaluate the accuracy of the analysis of any meteorological element in the "no-data" region, it was decided to test analytically known fields. The simplest and most convenient field which can be defined in space is that of the latitude and longitude of the grid points. We may assume various types of first guess of the latitudes and longitudes of these grid points and then make iterative corrections using the coordinates of the upper-air stations in the same way that was used to analyze the wind field. Of course, such tests are not necessarily equivalent to those for meteorological elements which have more complicated non-linear spatial distributions. Still, they have provided useful information for the purpose of removing distortions in the analyzed meteorological fields.

Figure 13 is a typical example of the "analyzed" latitude and longitude lines. Significant distortions are evident. After several tests with various sets of ν , $\gamma_m^{(\nu)}$, $b^{(\nu)}$, and $G^{(\nu)}$ and $\gamma_t^{(\gamma)}$, and with various forms of the first guess, a better set of parameters was chosen as described in the previous section. Use of equation (3)' considerably reduces the distortion of analyzed field. However, it was also realized that the exact first guess need not necessarily remain uncorrected, because the smoothing process involved in equation (3)' may add grid data distributed asymmetrically around the grid under consideration.

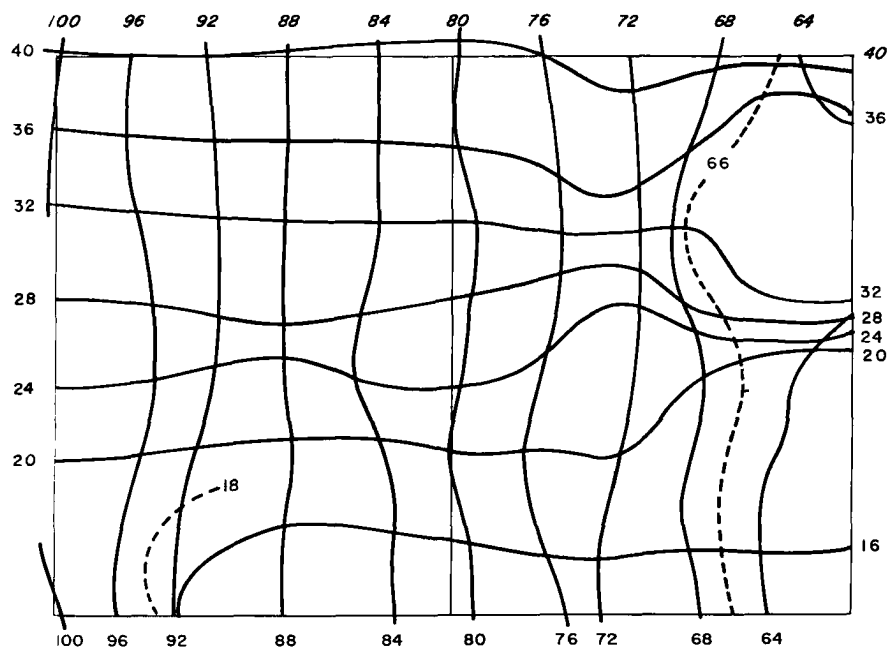


Fig. 13 Analyzed latitudinal and longitudinal lines by the correction method. ($\nu=1$, $\gamma_m=20.0$, $b=0.08$, $G=0.10$).

Two analyses of the latitude and the longitudinal lines with the parameters finally chosen are shown in Figures 14 and 15. These were obtained from two extreme first guesses, namely from 0 first guess and from the exact solution respectively.

3.4 Examples of Upper-Wind Analysis

Figures 16 and 17 are examples of the analyzed 500-mb winds presented in the same way as the surface wind. Figures 18 and 19 illustrate 200-mb wind fields. Agreement between observations and analyzed winds is fairly good. Resolution of shear lines, troughs, cols, waves and upper-level anticyclonic cells appears to be nearly satisfactory.

The machine time needed to get a complete series of the 10 level analysis was about 24 minutes per map time by CDC-3600.

3.5 Statistical Results of the Upper-Wind Analysis

Because of the large amount of machine time needed, only three map times could be tested. In Table 8, the correlation coefficients and the root mean square errors for the three cases are listed for each of the 10 levels analyzed.

TABLE 8 Correlation Coefficients and R.M.S. (kts) between the Observation and Analyzed Winds $|V|$ * (scalar velocity of vector resultant wind(kts))

map time ^{mb}	975	900	800	700	600	500	400	300	200	125
2300	0.841 3.03	0.934 2.87	0.884 4.04	0.906 3.19	0.914 3.23	0.949 3.46	0.966 3.65	0.969 4.33	0.960 5.17	0.962 3.58
2312	0.905 2.62	0.932 3.46	0.930 3.32	0.946 3.12	0.953 3.07	0.963 3.48	0.970 3.94	0.967 4.82	0.965 5.03	0.954 4.00
2400	0.861 2.96	0.896 3.28	0.891 3.31	0.914 3.32	0.936 3.19	0.970 2.90	0.979 3.29	0.967 5.49	0.952 7.05	0.956 4.14

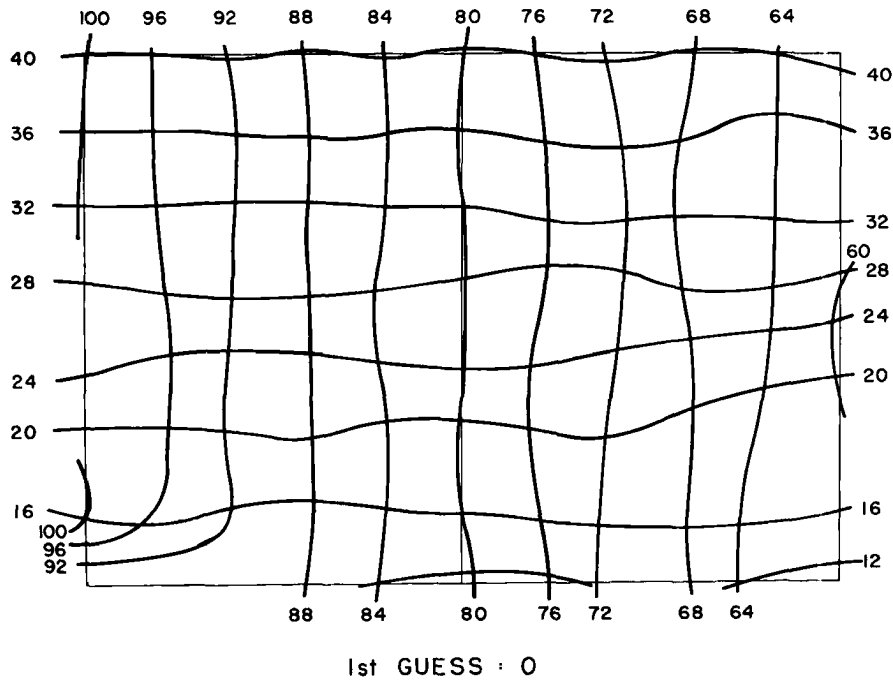


Fig. 14 Analyzed latitudinal and longitudinal lines by the final scheme ($\nu=3$, $\gamma_m=6.0$, $b=0.08$, $G=0.04$) started from the first guess 0.

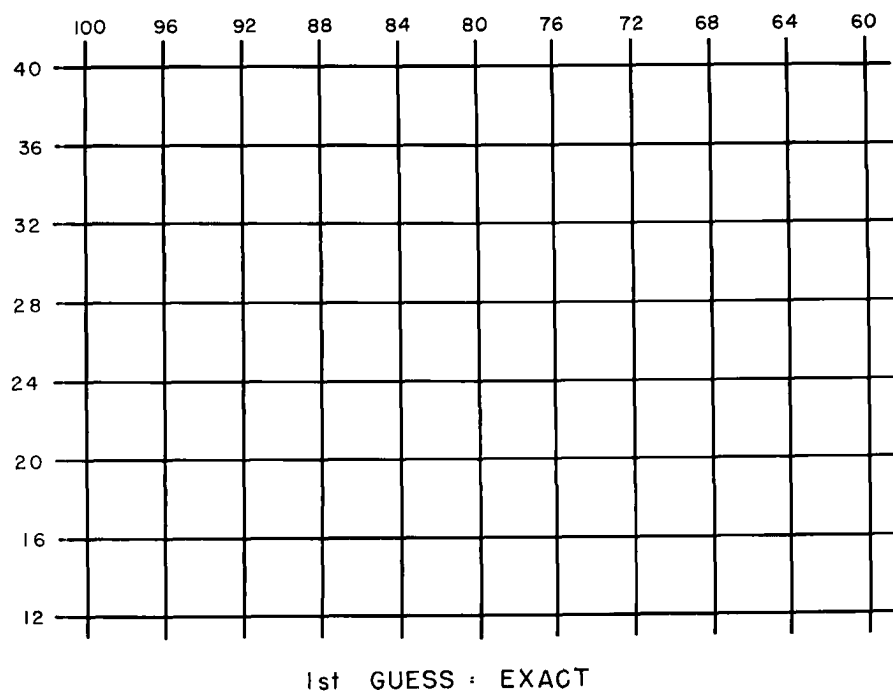


Fig. 15 Analyzed latitudinal and longitudinal lines by the final scheme but started from the exact first guess.

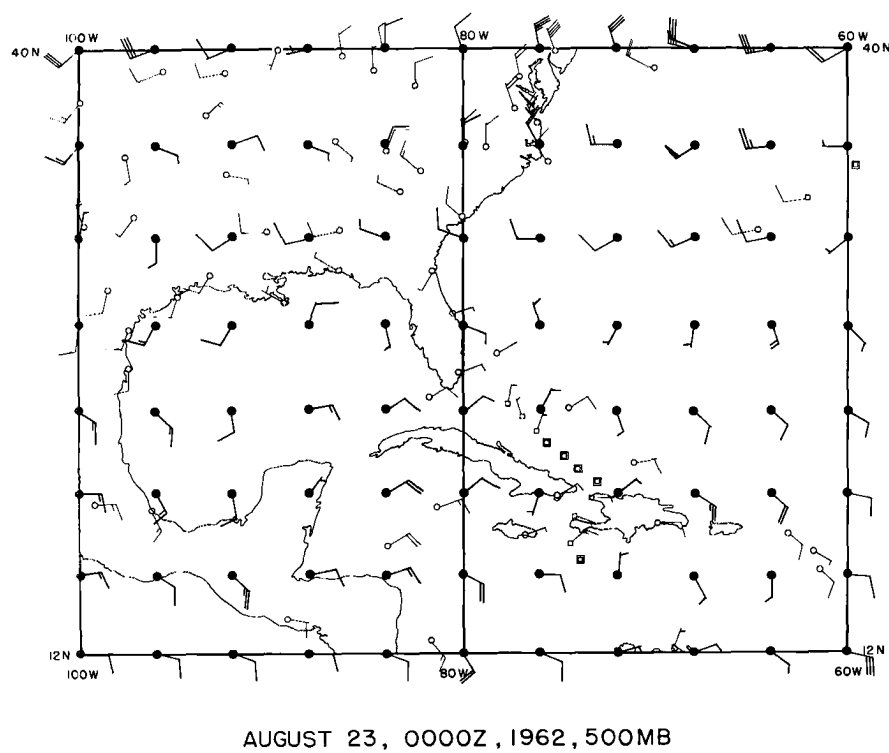
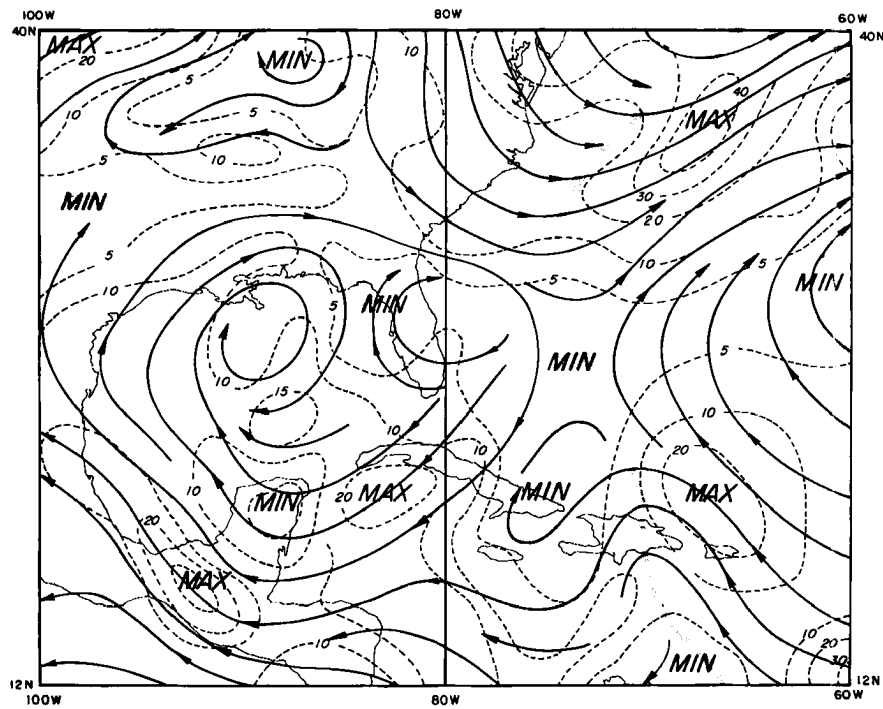
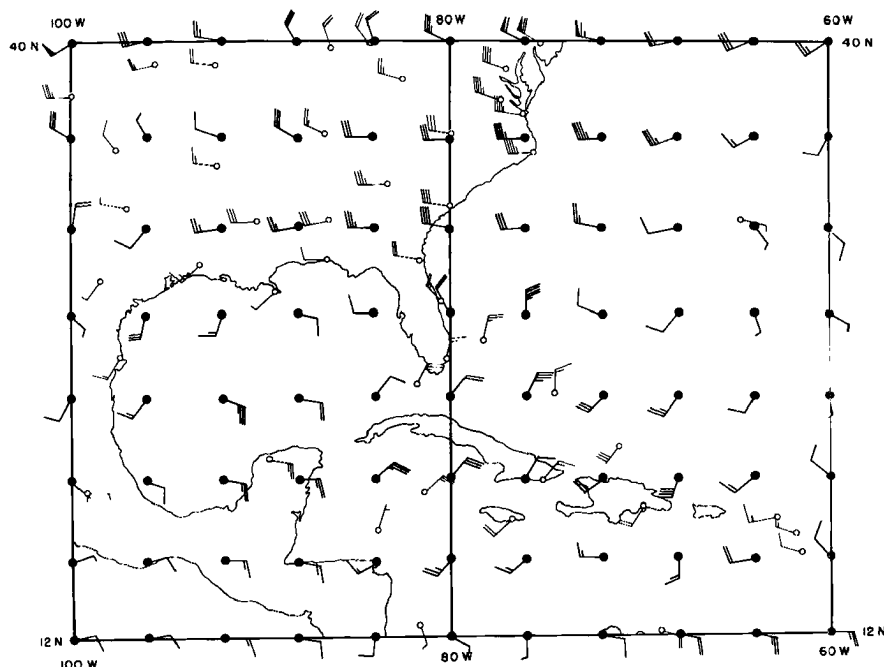


Fig. 16 Objective analysis of 500 mb-level wind.



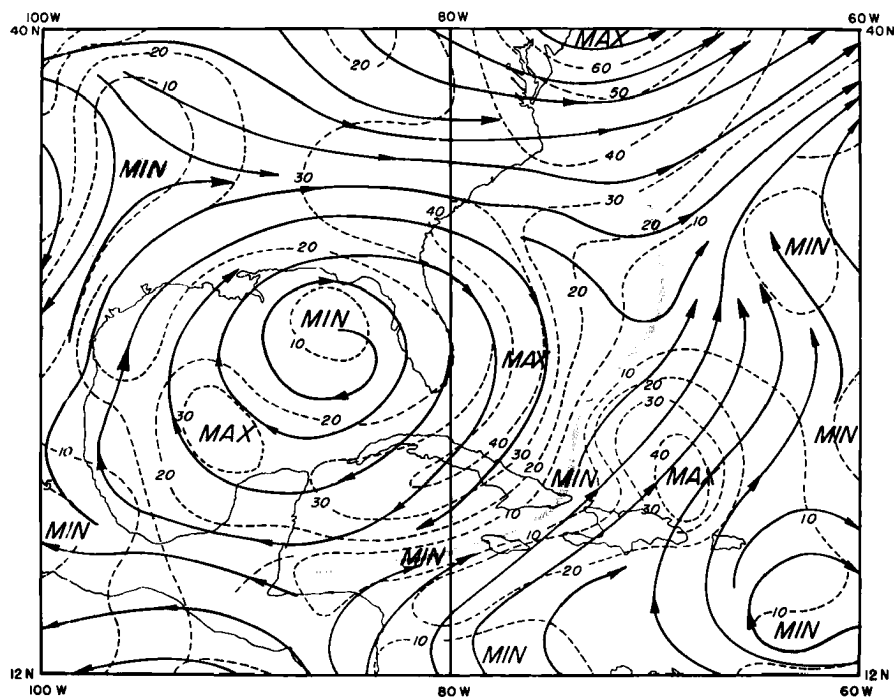
AUGUST 23, 0000Z, 1962, 500 MB

Fig. 17 Analysis of streamlines and isotachs (kts) at 500 mb based on the objective analysis.



AUGUST 23, 0000Z, 1962, 200MB

Fig. 18 Objective analysis of 200 mb-level wind.



AUGUST 23. 0000Z. 1962 . 200MB

Fig. 19 Streamlines and isotachs (5 kts) at 200 mb based on the objective analysis.

4. CONCLUSION AND REMARKS

From the results of this experimental study, the synoptic-scale objective analysis scheme appears to be feasible for the Caribbean region.

Further tests on the analysis scheme and expansion of the analysis for the upper-level temperature, moisture and the isobaric height data are planned. In order to make thoroughly satisfactory tests of the analyzed upper winds, it will be necessary to carry various computations on the vorticity, divergence and vertical motion.

ACKNOWLEDGEMENT

The study has been supported by a research contract between Dr. H. Riehl of Colorado State University and the National Hurricane Research Project, U. S. Weather Bureau, Miami, Florida. The author wishes to thank the interests and discussions given by Drs. H. Riehl, William Gray, and F. Baer of Colorado State University and Dr. S. L. Rosenthal of the National Hurricane Research Project. All the data were supplied from Dr. R. C. Gentry of the National Hurricane Research Project. Most of the machine computations were done by a CDC-3600 computer at the Computing Facility, National Center for Atmospheric Research, Boulder, Colorado. Technical assistance has been given by Mr. J. Connell. A large number of data have been processed and analyzed by Miss J. Bush, Mrs. M. Davis, Mrs. J. Mahlman and Miss N. Shima. Figures were drafted by Miss H. Akari.